

UC Berkeley

UC Berkeley Previously Published Works

Title

Follistatin interacts with Noggin in the development of the axial skeleton

Permalink

<https://escholarship.org/uc/item/6z9817zb>

Journal

Cells and Development, 131(1)

ISSN

2667-291X

Authors

Stafford, David A
Monica, Stefanie D
Harland, Richard M

Publication Date

2014-02-01

DOI

10.1016/j.mod.2013.10.001

Peer reviewed

Published in final edited form as:

Mech Dev. 2014 February ; 131: 78–85. doi:10.1016/j.mod.2013.10.001.

***Follistatin* interacts with *Noggin* in the development of the axial skeleton**

David A. Stafford, Stefanie D. Monica, and Richard M. Harland

Dept. of Molecular and Cell Biology and Center for Integrative Genomics, University of California, Life Sciences Addition, room 571, #3200 Berkeley, CA 94720, USA. Lab phone: (510) 643-7830. Lab fax: (510) 643-6791

Abstract

When compared to single mutants for *Follistatin* or *Noggin*, we find that double mutants display a dramatic further reduction in trunk cartilage formation, particularly in the vertebral bodies and proximal ribs. Consistent with these observations, expression of the early sclerotome markers *Pax1* and *Uncx* is diminished in *Noggin;Follistatin* compound mutants. In contrast, *Sim1* expression expands medially in double mutants. As the onset of *Follistatin* expression coincides with sclerotome specification, we argue that the effect of *Follistatin* occurs after sclerotome induction. We hypothesize that *Follistatin* aids in maintaining proper somite size, and consequently sclerotome progenitor numbers, by preventing paraxial mesoderm from adopting an intermediate/lateral plate mesodermal fate in the *Noggin*-deficient state.

Keywords

BMP antagonist; axial skeleton; sclerotome; mouse

Introduction

Bone morphogenetic protein (BMP) antagonists supply a critical permissive signal in sclerotome specification (Stafford et al., 2011). Elevated BMP signaling resulting from *Noggin* mutation results in the loss of caudal vertebrae (Brunet et al., 1998), while concurrent ablation of the BMP antagonist genes *Gremlin1* and *Noggin* result in a dramatic reduction in the expression of sclerotome-specific genes *Pax1*, *Pax9*, *Uncx*, and *Nkx3.2*, and a complete failure to form the axial skeleton. In contrast, embryos lacking *Gremlin1* alone have normal sclerotomes (Khokha et al., 2003), raising the possibility that other BMP antagonists that lack an overt axial skeletal phenotype may function in sclerotome induction. Once such gene with especially striking expression in the early somites is *Follistatin*.

Follistatin encodes a cysteine-rich protein that inhibits the activity of Activins and BMPs (Amthor et al., 2002; Fainsod et al., 1997; Hemmati-Brivanlou et al., 1994; Iemura et al., 1998; Michel et al., 1993) by antagonizing both type 1 and type 2 receptor binding (Thompson et al., 2005). *Follistatin* binds and inactivates Myostatin/GDF8, thereby

© 2013 Elsevier Ireland Ltd. All rights reserved.

Corresponding author dastaffo@berkeley.edu.

Publisher's Disclaimer: This is a PDF file of an unedited manuscript that has been accepted for publication. As a service to our customers we are providing this early version of the manuscript. The manuscript will undergo copyediting, typesetting, and review of the resulting proof before it is published in its final citable form. Please note that during the production process errors may be discovered which could affect the content, and all legal disclaimers that apply to the journal pertain.

permitting Pax3 and MyoD-mediated myogenesis (Amthor et al., 2004). Consistent with a role in promoting the skeletal muscle lineage, mice lacking the *Follistatin* gene exhibit diminished muscle mass (Matzuk et al., 1995). In addition, these mutants exhibit defects in the whiskers, hard palate, and teeth, and die at birth due to respiratory distress (Matzuk et al., 1995). *Follistatin* null mice also fail to form the most posterior, floating 13th rib, suggesting involvement in the anterior-posterior regionalization of the axial skeleton. However, in contrast to the skeletal defect observed in *Noggin* mutants, *Follistatin*-deficient mice do not display regions of axial skeletal agenesis or hypertrophy. *Follistatin* is expressed in somites, the mesodermal units that flank the neural tube and from which both the axial skeleton and skeletal muscle derive. Nevertheless, no role in somite patterning has been attributed to *Follistatin*. Using conditional alleles for *Noggin* and *Follistatin*, we tested the hypothesis that *Follistatin* might overlap in function with *Noggin* and contribute to development of the axial skeleton.

Material and Methods

Conditional alleles for *Noggin*, *Follistatin*, and *Gremlin1*, and the beta-actin promoter driven cre line were previously described (Jorgez et al., 2004; Stafford et al., 2011; Gazzero et al., 2007; Lewandoski et al., 1997). Alleles were maintained on a mice from a mixed C57/B6;129/Ola;FVB background. Whole mount in situ hybridization and Alcian Blue cartilage stains were performed as described (Khokha et al., 2003; Stafford et al., 2011). Quantitative PCR was performed on a BioRad CFX-100 Real Time System using the following primer sets (all annealing temperatures 60° C). *Chordin*: GAC TGC TGC AAA CAG TGT CCG TGT CC, ACT GAT GGG TGC CAG CTC T; *Follistatin*: CCT CCT GCT GCT GCT ACT CT, GGT GCT GCA AAC ACT CTT CCT; *Gapdh*: TTG ATG GCA ACA ATC TCC AC, CGT CCC GTA GAC AAA ATG GT; *Gremlin1*: ACA GCG AAG AAC CTG AGG AC, CCT TTC TTT TTC CCC TCA GC; *Meox1*: GAA GGC TGT CCT CTC CTT CC, CGG AGA AGA AAT CAT CCA GAA; *Noggin*: TGT ACG CGT GGA ATG ACC TA, GTG AGG TGC ACA GAC TTG GA; *Pax1*: GGC AGT CCG TGT AAG CTA CC, CAA TGA CCT TCA AAC ACC GA; *Uncx*: GGA GAA GGC GTT CAA TGA GA, CTT CTT TCT CCA TTT GGC CC.

Results

Follistatin is expressed in somites

Initiating at E6.5, *Follistatin* is expressed dynamically in the primitive streak, central nervous system and paraxial mesoderm (Albano and Smith, 1994). We stained WT mouse embryos between E8.5 and E10.0 for *Follistatin* to define expression in the developing trunk. We confirmed that *Follistatin* is expressed in paraxial mesoderm, with expression initiating throughout the epithelial somite shortly after somitogenesis (Fig.1A). As the newly formed somite undergoes initial pattern formation, *Follistatin* expression becomes concentrated in the dorsal lateral aspect of the somite(Fig.1B). By the time the somite is 30 hours old, *Follistatin* expression is restricted to the posterior aspect of the dermomyotome (Fig.1C).

We reasoned that the onset of *Follistatin* expression in the embryonic trunk is likely too late for *Follistatin* to function in initial somite patterning; the appearance of *Follistatin* transcript coincides with the onset of sclerotome and dermomyotome marker expression. In contrast, *Noggin* and *Gremlin1*, which together are required for sclerotome specification, are expressed well before somite formation. Nevertheless, the striking and dynamic expression of *Follistatin* during the specification of somite-derived tissues is consistent with a role in somite development. Although no somite abnormalities were described for embryos lacking *Follistatin* (Matzuk et al., 1995), the functional redundancy exhibited by other BMP

antagonists (Anderson et al., 2002; Bachiller et al., 2000; Stafford et al., 2011) led us to posit that loss of *Follistatin* may exacerbate the somite defects associated with loss of *Noggin*, the antagonist with the most severe somite phenotype. To test the hypothesis that *Follistatin* and *Noggin* interact genetically in somite development, we generated *Noggin;Follistatin* compound mutants.

We crossed females homozygous for conditional alleles for *Noggin* (Stafford et al., 2011) and *Follistatin* (Jorgez et al., 2004) to males heterozygous for these alleles and also homozygous for a transgene expressing Cre from the beta-actin promoter (Lewandoski et al., 1997). This approach produces equal numbers of each of the following genetic classes: $Nog^{fx/+};Fst^{fx/+}$, used as controls; $Nog^{fx/fx};Fst^{fx/+}$, *Noggin* mutants; $Nog^{fx/+};Fst^{fx/fx}$, *Follistatin* mutants; $Nog^{fx/fx};Fst^{fx/fx}$, double mutants. Quantitative PCR from genomic DNA confirmed that embryos bearing two conditional alleles retained less than 0.003% of inter-floxed DNA for *Noggin* and *Follistatin*, indicating successful, ubiquitous gene ablation. Moreover, as discussed below, homozygous mutant embryos displayed previously described *Noggin* and *Follistatin* null mutant phenotypes.

Follistatin interacts genetically with Noggin in axial skeleton development

As our primary interest lies in the role of BMP antagonist genes in axial skeleton development, we first compared the morphologies of ribs, vertebrae, and spinous processes in the different genetic classes by whole-mount alcian blue staining at E13.5 (Fig.2). $Nog^{fx/+};Fst^{fx/+}$ skeletons exhibit normal axial skeleton morphology. While the skeletal elements of $Nog^{fx/+};Fst^{fx/fx}$ specimens were properly articulated and had normal length and diameter, in 4 of 5 skeletons the 13th rib was absent, consistent with the description of the *Follistatin* null animals (Fig. 2B; Matzuk et al., 1995). As we previously reported, embryos lacking only *Noggin* exhibited hyperplasia of the thoracic ribs and vertebrae, absent cartilage in the lumbar region, and a reappearance of vertebral bodies at the level of the pelvis (Fig. 2C; Stafford et al., 2011). Deletion of one or both copies of *Follistatin* dramatically increased the severity of the *Noggin* axial skeleton phenotype. The position of the most posterior axial skeletal element in $Nog^{fx/fx};Fst^{fx/+}$ examples was further anterior than in $Nog^{fx/fx}$ examples (Fig 2, compare arrows.). Furthermore, the halves of vertebral bodies were misaligned in all 4 $Nog^{fx/fx};Fst^{fx/+}$ specimens examined. Ablation of both copies of *Follistatin* enhanced the defects of the medial axial skeleton. The vertebral bodies in $Nog^{fx/fx};Fst^{fx/fx}$ were reduced (4 of 4; Fig 2E). In addition, the diameter of the proximal ribs was diminished in comparison to distal ribs. From our examination of these skeletons, we conclude that loss of *Follistatin* enhances the *Noggin* skeletal phenotype and that the midline aspects of the axial skeleton, including vertebral bodies and proximal ribs, are the more severely affected elements. *Pax1* and *Pax9* function together in the formation of the vertebral column (Peters et al., 1999) while *Uncx* is required for pedicles, transverse processes, and proximal ribs (Leitges et al., 2000). We hypothesized that if the loss of *Follistatin* in *Noggin* mutants enhances deficiencies in more medial aspects of the axial skeleton, the expression of genes required for these elements may be most affected. We therefore analyzed *Pax1* and *Uncx* expression in $Nog^{fx/+};Fst^{fx/+}$ (controls), $Nog^{fx/+};Fst^{fx/fx}$, (*Follistatin* mutant-*Noggin* heterozygotes), $Nog^{fx/fx};Fst^{fx/+}$, (*Noggin* mutant-*Follistatin* heterozygotes) and $Nog^{fx/fx};Fst^{fx/fx}$ (double mutants) at E9.5 by whole-mount in situ hybridization (WM-ISH; Fig. 3). Expression of both *Pax1* and *Uncx* in *Follistatin*-deficient embryos was the same as in controls. However, as copies of *Follistatin* were removed from *Noggin* mutants, the posterior limit of *Pax1* (n = 3) and *Uncx* (n = 3) expression became restricted to increasingly anterior positions. Nevertheless, while the signal was diminished, *Noggin;Follistatin* double mutant embryos still expressed *Pax1* and *Uncx*. To measure subtle changes in somite marker activity, we performed quantitative RT-PCR (Sup. Fig. 1). This analysis confirmed that loss of *Follistatin* does marginally reduce *Pax1* and *Uncx* compared to loss of *Noggin* alone.

However, if *Pax1* and *Uncx* expression is expressed as a percentage of a general paraxial mesoderm marker, in this case *Meox1*, the loss of *Follistatin* does not further reduce *Pax1*. Thus the diminished *Pax1* and *Uncx* transcript levels are a result of a reduction in paraxial mesoderm.

Generally, the distal ribs in *Follistatin;Noggin* compound mutants were the least severely affected elements of the axial skeleton. Surprisingly, *Nog^{fx/fx};Fst^{fx/fx}* double mutants sometimes exhibited condensations in the lateral lumbar region (3 of 5), some of which had the appearance of ribs. The origins of the distal ribs are controversial. One embryological study using chick and quail chimeras suggests that progenitors in the lateral dermomyotome give rise to the distal ribs (Kato and Aoyama, 1998). Consistent with this analysis, genetic ablation of the *Myf5* lineage results in severe distal rib defects, although this may result from transient *Myf5* expression in pre-somitic mesoderm or be a non-cell autonomous effect resulting from the absence of an inductive interaction supplied by lateral dermomyotome (Haldar et al., 2008). A second avian chimera study using smaller grafts concluded that distal ribs are indeed a derivative of the sclerotome (Huang et al., 2000). While imperfectly understood, it is clear that lateral domains of the somite are critical for normal axial skeleton formation. We therefore analyzed *Myf5* expression in *Noggin;Follistatin* compound mutants. We observed no changes in *Myf5* expression in E10.5 *Noggin*-mutants upon removal of one of both copies of *Follistatin*, consistent with our observation that the medial derivatives are the most severely affected features of *Nog^{fx/fx};Fst^{fx/fx}* double mutant skeletons (Sup. Fig. 2).

Noggin;Follistatin somites are smaller and lateralized

The diminished levels of sclerotome gene expression, particularly in domains destined to contribute to more medial elements of the axial skeletal, could be caused by elevated cell death or reduced proliferation in these lineages. To define the contribution of these processes, we performed TUNEL and phosphorylated histone-3 (PH3) on sections cut from the anterior-posterior level of somite 12-16 in E9.5 embryos of each genetic class. Trunk segments from at least 3 separate embryos from each genetic class were analyzed. Essentially no TUNEL positive cells were detected in paraxial mesoderm; most sections had none (not shown). We did observe previously described dorsal neural tube signal in embryos of all classes lacking *Noggin* (McMahon et al., 1998; Stafford et al., 2011), demonstrating efficacy of the assay. To define proliferation rates in the paraxial mesoderm between the different classes, we counted PH3+ nuclei and expressed these as a function of total nuclei. We restricted our counts to the morphologically defined somite. After analyzing a minimum of 11 sections from at least 3 embryos of each genotype, we found that the overall mitosis rates were not statistically different; about 3% of cells are mitotic regardless of genetic class (not shown). A caveat to our approach is that we had no way of counting sclerotome exclusively in our sections. However, we could find no indication of a difference in proliferation rate between genotypes at the stages we examined.

The most striking difference between the somites of the different genotypes was the overall quantity of paraxial mesoderm; in comparison to controls and *Follistatin* mutants (Fig. 4A,B), *Noggin* and *Noggin* mutant-*Follistatin* heterozygotes exhibited significantly smaller thoracic trunk somites (Fig.4C,D). The somites of embryos lacking both genes were smaller still (Fig.4E). A complication of these analyses was the relative smaller size of antagonist-mutant embryos. To account for the size differences in between embryos of different genotypes, we compared the area of the neural tube, somite, midgut and somatic lateral plate in E9.5 sections collected just posterior to the forelimb. We found the total area of embryonic tissue in sections cut from specimens lacking *Noggin* and *Follistatin* was less than half that of controls, and exhibited a reduction in all tissues examined except for midgut. However, in double mutants, the somite was affected most; somite area was only

15% of the embryo, compared to 34% and 27% for controls and *Noggin* mutants, respectively. In contrast, the lateral plate mesoderm represented a proportionally greater amount of *Noggin;Follistatin* double mutant embryos, comprising 57% of the embryo, in contrast to 41% in controls. While the effect of *Noggin* ablation on somite size has been described (McMahon et al., 1998; Stafford et al., 2011), we were surprised that deletion of *Follistatin* enhanced this phenotype, as *Follistatin* expression initiates after somite formation. The overall diminished size of trunk structures in *Noggin;Follistatin* double mutant embryos may also be a consequence of diminished *Follistatin* expression in extraembryonic tissues. *Follistatin* expression has been reported in E7.5 parietal endoderm (Albano and Smith, 1994). We examined the expression of four BMP antagonist genes, *Noggin*, *Follistatin*, *Gremlin1*, and *Chordin*, in the E9.5 ectoplacental cone (Sup. Fig. 3). *Follistatin* expression was four-fold higher than the next highest expressed gene, *Noggin*, consistent with a role in placental function. Nevertheless, the proportionally larger lateral mesoderm and smaller paraxial mesoderm indicates a patterning defect. The absence of any overt proliferation differences raised the possibility that even after somites form, cells may continue to be influenced in their allocation to non-segmented lateral populations.

To access the lateral identity of paraxial mesoderm in *Noggin;Follistatin* compound mutants, we examined expression of the transcriptional repressor *Sim1*. *Sim1* is expressed in the intermediate mesoderm of the posterior trunk and has been shown to expand medially when BMP signaling is elevated by removing *Noggin* (Wijgerde et al., 2005). We observed bilateral *Sim1* expression posterior to the forelimb in all classes. In controls and *Follistatin*-deficient embryos, this expression was restricted to characteristic discrete stripes representing the intermediate mesoderm lateral to the morphologically distinct somites (Fig. 5A-B). As was observed in Wijgerde, et al., embryos lacking *Noggin* displayed a medial expansion of *Sim1* into the lateral somite (4 of 4; Fig. 5C). This lateralization was further enhanced in *Noggin;Follistatin* double mutants, with expression extending in some cases to the neural tube (2 of 3; Fig. 5D). Ectopic *Sim1* expression in the paraxial mesoderm is consistent with a model in which the loss of BMP antagonists results in a smaller population of progenitors competent to form axial skeleton.

Taken together, our analysis of axial cartilage, somitic marker expression, and paraxial mesoderm size led us to hypothesize that the early sclerotome in *Noggin* mutants remains competent to be lateralized, and *Follistatin* functions to prevent this from occurring. These results suggest that medial-lateral mesoderm patterning continues over time and that even after somites form and assume their initial gene expression patterns they can take on the identity of more lateral mesodermal cell types.

BMP does not inhibit Follistatin activation

Our original interest in *Follistatin* stemmed from our previously unpublished observation that *Follistatin* transcript levels are reduced in *Noggin;Gremlin1* compound mutant trunks at E9.0, suggesting that activation of *Follistatin* may require inhibition of BMP signaling. However, when we compared *Follistatin* expression in *Noggin;Gremlin1* double mutants to other genetic classes at E9.0, there was no apparent qualitative difference in signal (Fig. 6A-D). Quantitative RT-PCR did reveal a 50% reduction of *Follistatin* transcript levels in *Noggin;Gremlin1* double mutants when compared to *Gapdh* (Fig. 6E). However, this was not observed when *Follistatin* transcript levels were normalized to those of *Meox1*, a general marker of paraxial mesoderm (Fig. 6F). In contrast, *Pax1*, which is expressed minimally in embryos lacking *Noggin* and *Gremlin* (Stafford et al., 2011), is reduced relative to *Meox1* (Fig. 6G). We interpret the diminished *Follistatin* in *Noggin;Gremlin1* compound mutants as a consequence of an overall reduction in somitic size (McMahon et al., 1998).

These data suggest that the elevated BMP does not interfere with *Follistatin* activation. Indeed, BMP may promote *Follistatin* expression in the somite.

Discussion

Of the different BMP antagonists, loss of *Noggin* has the most severe effect on the patterning of the axial skeleton. Nevertheless, recent analysis of compound *Noggin* and *Gremlin* mutants has revealed the contributions of other BMP antagonist genes. Here we present evidence that *Follistatin* functions to maintain paraxial mesoderm identity during early somite-patterning events. Coincident with the activation of *Follistatin* in the regionalizing somite, the expression of *Noggin* and *Gremlin1* diminishes. Thus, there is a “BMP antagonist relay” in early sclerotome development.

In the chick, application of *Noggin* to the presumptive lateral plate mesoderm results in ectopic somites (Tonegawa and Takahashi, 1998). Similarly, loss of an allele of *BMP4* ameliorates the lateralization of the paraxial mesoderm observed in *Noggin* mutant embryos (Wijgerde et al., 2005). We show that the additional loss of *Follistatin* causes *Noggin*-deficient somitic tissue to more extensively adopt intermediate/lateral late mesoderm identity, which is consistent with a persistent function for BMP/BMP antagonist signaling during the differentiation of somite derivatives. Moreover, our analysis provides a surprising insight into the duration during which medial-lateral identity can be specified. Our data here suggest that even after a somite is formed, elevated BMP can reassign paraxial mesoderm to a lateral, non-segmented fate.

In all antagonist-deficient embryos, the severity of the paraxial mesoderm phenotype increases posteriorly. A likely explanation is that BMPs secreted from lateral mesoderm and extra-embryonic sources are concentrated in the posterior (McMahon et al., 1998), and therefore the repercussions of decreased antagonist activity are more severe. In addition, we propose that morphology of the developing embryo contributes to this phenomenon; the lumbar region of the embryo is thinner than the thoracic region, and laterally-derived BMPs have less distance to diffuse to reach sensitive somitic precursors. Consistent with this interpretation, in mouse strains that exhibit a more mild *Noggin* phenotype, somite markers are expressed in the pelvic region (Stafford et al., 2011). Our work adds to existing data that indicates that in embryos with elevated BMP signaling, somites are smaller and lost posteriorly because cells are aberrantly specified as IM/LPM.

Follistatin expression in the somites is conserved in the vertebrates. In addition to those of amniotes, *Follistatin* homologues are expressed in the somites of salmon, zebrafish, and lamprey (Bauer et al., 1998; Hammond et al., 2009; Macqueen and Johnston, 2008). Axial skeleton formation in teleosts varies across species, and may not exist at all in agnathans (Ogasawara et al., 2000), although irregular axial cartilaginous condensations that may reflect primitive skeletal elements have been described. This argues against an ancestral role for somitic *Follistatin* in sclerotome formation. Also, either notochord or *Shh* interferes with somitic *Follistatin* expression, which is the opposite activity predicted for sclerotome-promoting genes (Amthor et al., 1996). This activity may not be direct, and might best be interpreted as a *Hh*-mediated inhibition of the myogenic lineage; high levels of *Shh* blocks *Wnt*-mediated dermomyotome induction (Marcelle et al., 1997). Nevertheless, our data clearly demonstrate that the axial skeleton is more severely affected in *Noggin;Follistatin* embryos vs. embryos lacking *Noggin* alone. We propose that across vertebrates, *Follistatin* normally functions to control *TGF-beta*-mediated proliferation and differentiation of the muscle progenitors of the dermomyotome (Amthor et al., 2004; Manceau et al., 2008). In the *Noggin*-mutant state, *Follistatin* can resist lateralization of paraxial mesoderm by BMP, thus

explaining the increased severity of axial skeletal deficiencies observed in *Noggin;Follistatin* double mutants.

Supplementary Material

Refer to Web version on PubMed Central for supplementary material.

Acknowledgments

We thank Debbie Pangilinan for animal care. This work is supported by NIH GM49346.

References

- Albano RM, Smith JC. Follistatin expression in ES and F9 cells and in preimplantation mouse embryos. *Int. J. Dev. Biol.* 1994; 38:543–547. [PubMed: 7848838]
- Amthor H, Connolly D, Patel K, Brand-Saberi B, Wilkinson DG, Cooke J, Christ B. The expression and regulation of follistatin and a follistatin-like gene during avian somite compartmentalization and myogenesis. *Dev. Biol.* 1996; 178:343–362. [PubMed: 8812134]
- Amthor H, Nicholas G, McKinnell I, Kemp CF, Sharma M, Kambadur R, Patel K. Follistatin complexes Myostatin and antagonises Myostatin-mediated inhibition of myogenesis. *Dev. Biol.* 2004; 270:19–30. [PubMed: 15136138]
- Bauer H, Meier A, Hild M, Stachel S, Economides A, Hazelett D, Harland RM, Hammerschmidt M. Follistatin and noggin are excluded from the zebrafish organizer. *Dev. Biol.* 1998; 204:488–507. [PubMed: 9882485]
- Brunet LJ, McMahon JA, McMahon AP, Harland RM. Noggin, cartilage morphogenesis, and joint formation in the mammalian skeleton. *Science.* 1998; 280:1455–1457. [PubMed: 9603738]
- Gazzerro E, Smerdel-Ramoya A, Zanotti S, Stadmeier L, Durant D, Economides AN, Canalis E. Conditional deletion of gremlin causes a transient increase in bone formation and bone mass. *J. Biol. Chem.* 2007; 282:31549–31557. [PubMed: 17785465]
- Hammond KL, Baxendale S, McCauley DW, Ingham PW, Whitfield TT. Expression of patched, *prdm1* and *engrailed* in the lamprey somite reveals conserved responses to Hedgehog signaling. *Evol. Dev.* 2009; 11:27–40. [PubMed: 19196331]
- Huang R, Zhi Q, Schmidt C, Wilting J, Brand-Saberi B, Christ B. Sclerotomal origin of the ribs. *Development.* 2000; 127:527–532. [PubMed: 10631173]
- Jorgez CJ, Klysik M, Jamin SP, Behringer RR, Matzuk MM. Granulosa cell-specific inactivation of follistatin causes female fertility defects. *Mol. Endocrinol.* 2004; 18:953–967. [PubMed: 14701941]
- Khokha MK, Hsu D, Brunet LJ, Dionne MS, Harland RM. Gremlin is the BMP antagonist required for maintenance of Shh and Fgf signals during limb patterning. *Nat. Genet.* 2003; 34:303–307. [PubMed: 12808456]
- Lewandoski M, Meyers EN, Martin GR. Analysis of Fgf8 gene function in vertebrate development. *Cold Spring Harb. Symp. Quant. Biol.* 1997; 62:159–168. [PubMed: 9598348]
- Macqueen DJ, Johnston IA. Evolution of follistatin in teleosts revealed through phylogenetic, genomic and expression analyses. *Dev. Genes Evol.* 2008; 218:1–14. [PubMed: 18074148]
- Manceau M, Gros J, Savage K, Thomé V, McPherron A, Paterson B, Marcelle C. Myostatin promotes the terminal differentiation of embryonic muscle progenitors. *Genes Dev.* 2008; 22:668–681. [PubMed: 18316481]
- Marcelle C, Stark MR, Bronner-Fraser M. Coordinate actions of BMPs, Wnts, Shh and noggin mediate patterning of the dorsal somite. *Development.* 1997; 124:3955–3963. [PubMed: 9374393]
- McMahon JA, Takada S, Zimmerman LB, Fan CM, Harland RM, McMahon AP. Noggin-mediated antagonism of BMP signaling is required for growth and patterning of the neural tube and somite. *Genes Dev.* 1998; 12:1438–1452. [PubMed: 9585504]
- Ogasawara M, Shigetani Y, Hirano S, Satoh N, Kuratani S. Pax1/Pax9-Related genes in an agnathan vertebrate, *Lampetra japonica*: expression pattern of LjPax9 implies sequential evolutionary events toward the gnathostome body plan. *Dev. Biol.* 2000; 223:399–410. [PubMed: 10882524]

- Stafford DA, Brunet LJ, Khokha MK, Economides AN, Harland RM. Cooperative activity of noggin and gremlin 1 in axial skeleton development. *Development*. 2011; 138:1005–1014. [PubMed: 21303853]
- Tonegawa A, Takahashi Y. Somitogenesis controlled by Noggin. *Dev. Biol.* 1998; 202:172–182. [PubMed: 9769170]
- Wijgerde M, Karp S, McMahon J, McMahon AP. Noggin antagonism of BMP4 signaling controls development of the axial skeleton in the mouse. *Dev. Biol.* 2005; 286:149–157. [PubMed: 16122729]

Highlights

- Loss of *Follistatin* enhances *Noggin* mutant axial skeleton defects
- In *Noggin* mutants, *Follistatin* aids in maintaining proper somite size
- *Follistatin* affects somite size following somite formation
- *Follistatin* limits BMP-mediated lateralization of paraxial mesoderm
- *Noggin* and *Gremlin1* mutation does not reduce somitic *Follistatin* activation

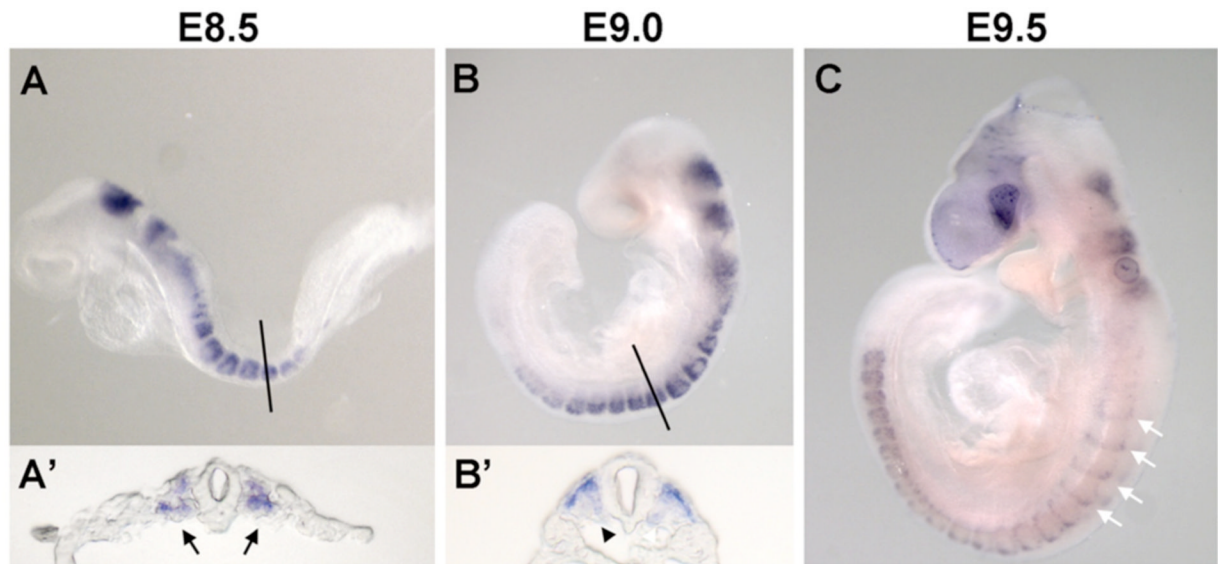


Fig. 1. *Follistatin* expression during somite pattern formation

Whole mount *in situ* hybridizations for *Follistatin*, lateral views. (A) E8.5 *Follistatin* expression in the newly-formed somites and hindbrain. (A') Magnified transverse view at the level of the line in panel A embryo showing *Follistatin* expression throughout the somite (arrows). (B) *Follistatin* expression becomes restricted to the dermomyotome. (B') Magnified transverse view of dermomyotome expression of *Follistatin* at the level of the black in panel B embryo; note decreased signal in the sclerotome (arrowhead). (C) At E9.5, *Follistatin* expression is detectable in the posterior dermomyotome (white arrows).

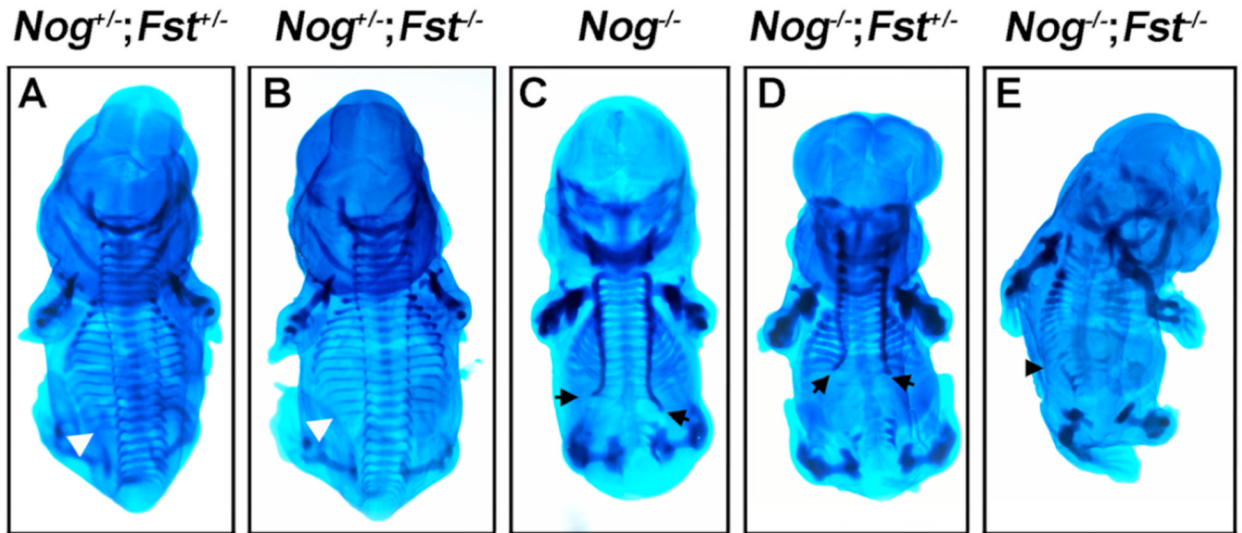


Fig. 2. Follistatin enhances the *Noggin* mutant skeletal phenotype

Whole mount E13.5 embryos stained with alcian blue to detect cartilage, dorsal views.

Nog^{fx/+};*Fst*^{fx/+} (A) differ from *Nog*^{fx/+};*Fst*^{fx/fx} (B) examples differ only in the absence of the 13th rib (arrowheads). (C) A *Nog*^{fx/fx} mutant displaying thickened cervical and thoracic skeletal elements and reduced lumbar cartilage. (D) In *Nog*^{fx/fx};*Fst*^{fx/+} animals, formation of the cartilage of the axial skeleton arrests at a more anterior aspect of the embryo. (E) Deletion of both *Follistatin* and *Noggin* results in an almost complete loss of the medial aspects of the centrum, processes, and proximal ribs.

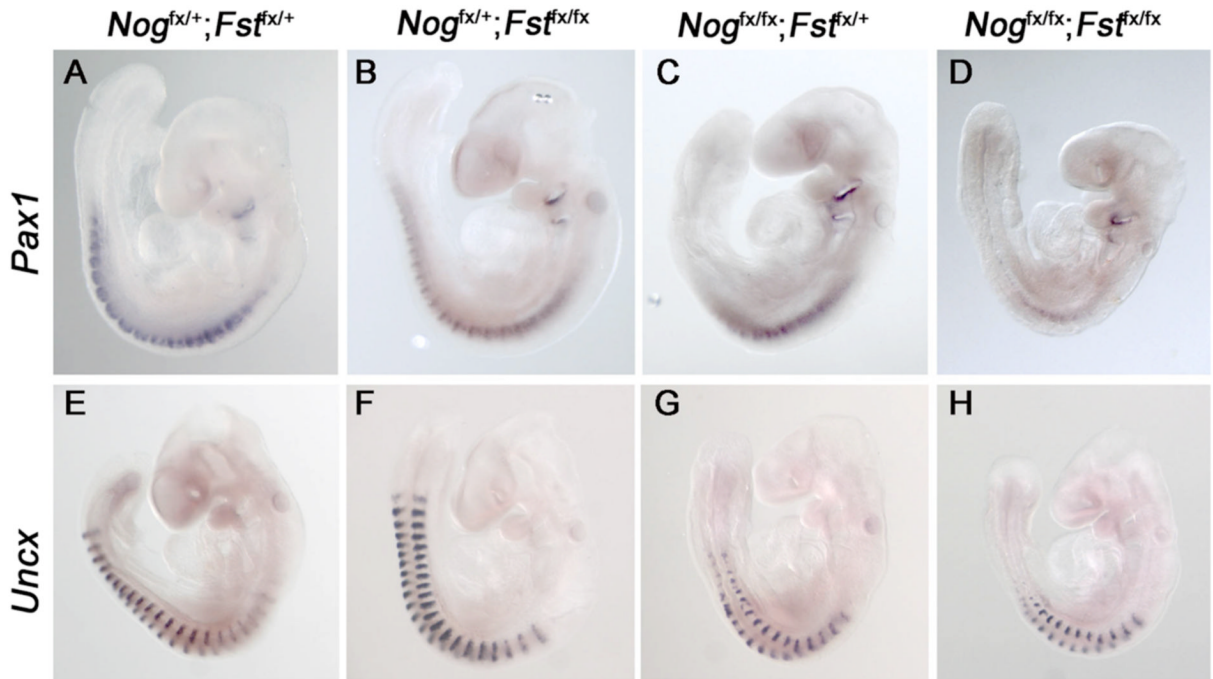


Fig. 3. Sclerotome marker expression is diminished in *Noggin*;*Follistatin* mutants
 E9.5 Whole mount *in situ* hybridizations for *Pax1* (A-D) and *Uncx* (E-H), lateral views. *Nog^{fx/+};Fst^{fx/+}* (A, E) and *Nog^{fx/+};Fst^{fx/fx}* (B, F) expressed *Pax1* (A, B) and *Uncx* (E, F) normally. (C, G) *Nog^{fx/fx};Fst^{fx/+}* specimens exhibit reduced level of both transcripts in the presumptive lumbar region. In *Nog^{fx/fx};Fst^{fx/fx}* animals, the posterior limit of expression was somite 10 for *Pax1* (D) and somite 14 for *Uncx* (H).

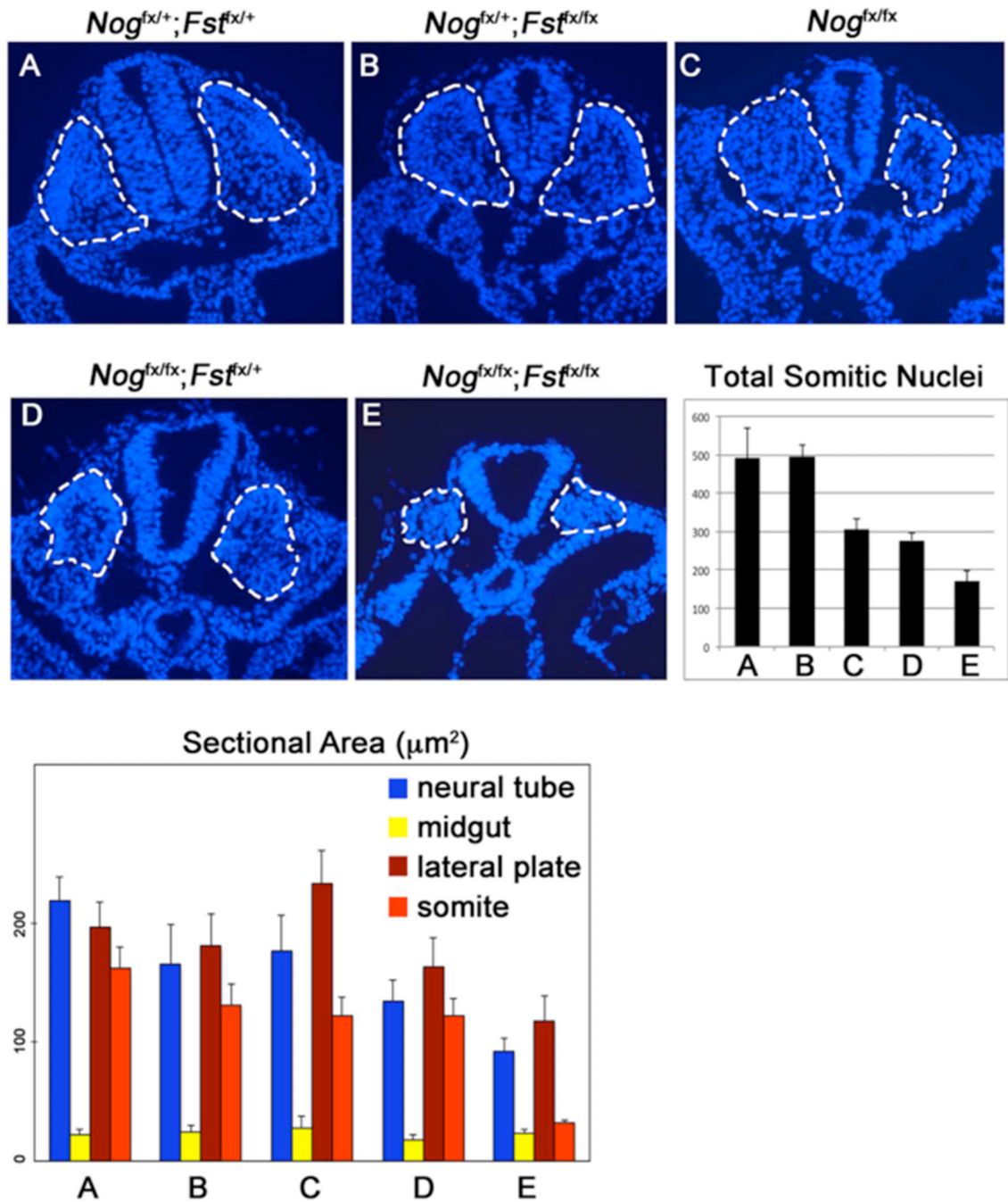


Fig. 4. Loss of *Noggin* and *Follistatin* results in smaller somites

(A-E) 12 μm sections were collected from the E9.5 trunk posterior to the forelimb and stained with hoechst. These were delineated with the dashed line and counted. (Total Somitic Nuclei) Histogram summarizing somite size for the different genetic classes. Somites in *Nog^{fx/+};**Fst^{fx/+}* and *Nog^{fx/+};**Fst^{fx/fx}* embryos (A, B) have significantly more cells than *Nog^{fx/fx}* and *Nog^{fx/fx};**Fst^{fx/+}* examples (C, D; $P < 0.0001$). These in turn have significantly more cells than *Nog^{fx/fx};**Fst^{fx/fx}* animals (E; < 0.0001). (Sectional Area) Histogram summarizing comparison of the area of different embryonic structures in transverse sections of the trunk. Regions were scored by morphology, bars in both graphs

indicate $2\times$ standard error, and a minimum of 5 sections cut from at least 3 embryos of each class were quantified.

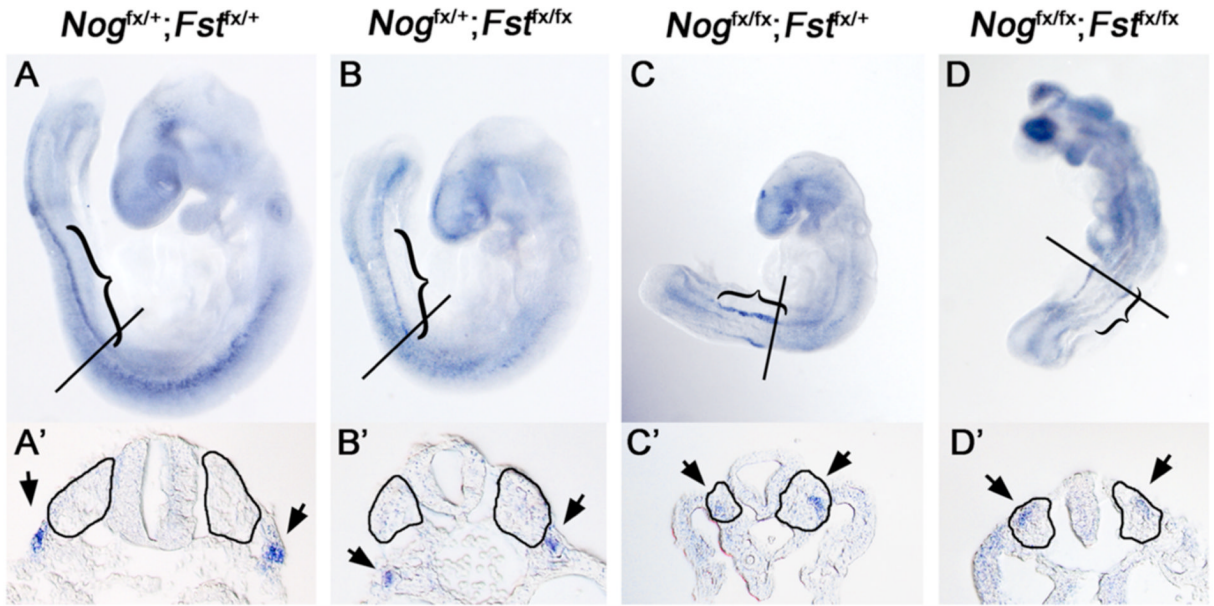


Fig. 5. *Sim1* expands medially in *Noggin*;*Follistatin* double mutants

E9.5 Whole mount *in situ* hybridizations for *Sim1*, lateral views (A-D) and transverse sections at the level of the line. (A'-D'). (A, B) In *Nog*^{f^x/+};*Fst*^{f^x/+} and *Nog*^{f^x/+};*Fst*^{f^x/fx} embryos, *Sim1* is expressed in the thoracic somites and the intermediate mesoderm (brackets). (A', B') shows the position of the signal lateral to the somite (arrowheads). (C) *Nog*^{f^x/fx};*Fst*^{f^x/+} specimens exhibit a broader *Sim1* expression domain that extends medially into the paraxial mesoderm (C'). *Nog*^{f^x/fx};*Fst*^{f^x/fx} animals (D, D') exhibit further medial expansion of *Sim1* expression.

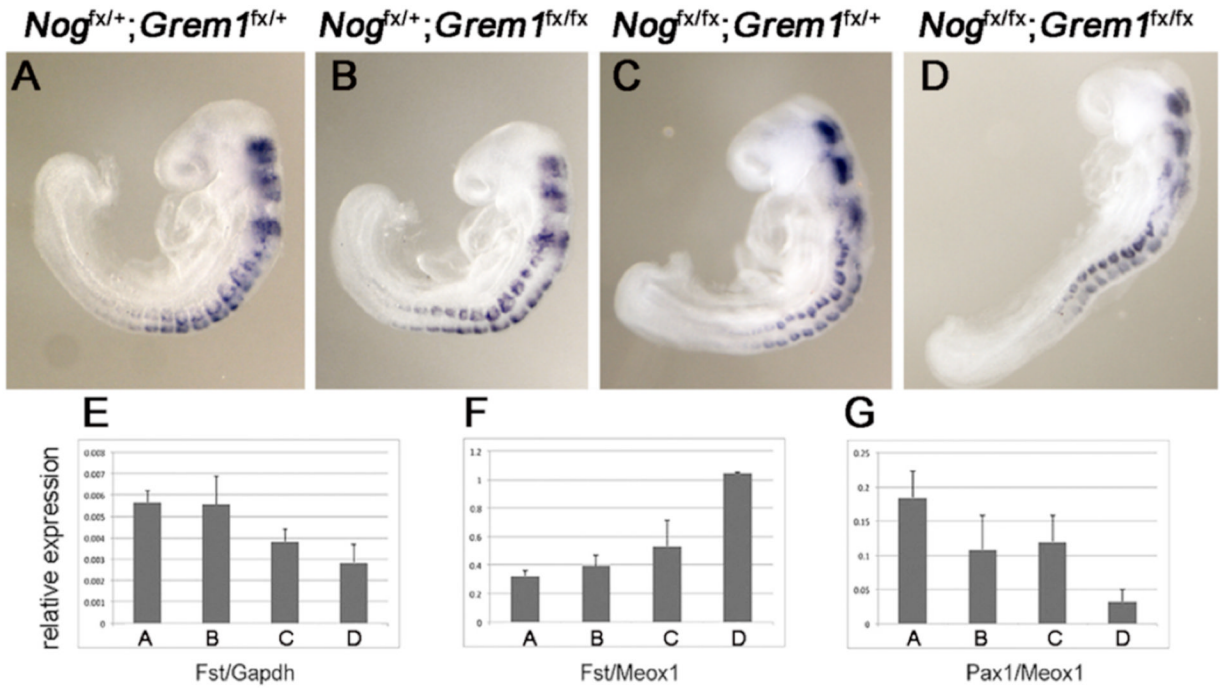


Fig. 6. Somitic *Follistatin* is elevated in *Noggin;Gremlin1* double mutants
 E9.5 Whole mount *in situ* hybridizations for *Fst*, lateral views (A-D). (A) $Nog^{fx/+};Grem1^{fx/+}$ controls, (B) $Nog^{fx/+};Grem1^{fx/fx}$ *Gremlin1* mutants, (C) $Nog^{fx/fx};Grem1^{fx/+}$ *Noggin* mutants, and (D) $Nog^{fx/fx};Grem1^{fx/fx}$ *Noggin;Gremlin1* double mutants all express *Follistatin*. (E-G) Histograms reporting quantitative PCRs. (E) Relative to expression of *Gapdh*, *Follistatin* is modestly reduced in *Noggin* and *Noggin;Gremlin1* double mutants. (F) When expressed as a function of transcript levels of *Meox1*, a general marker of the somite, *Follistatin* is elevated. (G) In contrast, *Pax1*, a gene that requires *Noggin* and *Gremlin1* for expression, is diminished. Bars indicate 2x standard error.